IMU Based Attitude Estimation in the Presence of Narrow-band Noise with Application to a Three-Axis Gimbal System

Guozheng Lu[1] and Fu Zhang[2]

In this paper, we consider the inertial measurement units (IMUs)-based attitude estimation, a common core problem in a large variety of robotic systems. In particular, we focus on the case where the IMU measurements are contaminated by narrow-band vibration noises caused by the system flexible mode, aerodynamic turbulence, or rotating parts (e.g. motors). Our proposed scheme is a complete solution to adaptively estimate the narrow-band noise and actively compensate it in the attitude estimation. More specifically, the scheme adopts a notch filter to attenuate the narrow-band noise and subsequently embeds such filter into a multiplicative extended Kalman filter (MEKF) framework to eliminate the induced transient error. Furthermore, a least mean square (LMS) method is utilized to estimate the dominant noise frequency in real time, forming an adaptive notch filter that can effectively attenuate narrow-band noise with time-varying dominant frequency. The complete algorithm is verified on an actual gimbal system with exhaustive experiments.

I. Introduction

Attitude estimation, determining the orientation of a rigid body from a series of non-ideal and noisy sensors, is a fundamental task in the robot attitude control, such as unmanned aerial vehicles (UAVs) [1] and multi-axis gimbal system [2]. Attitude are generally measured by or resolved from two types of sensors: 1) line-of-sight attitude sensors by which vehicle's attitude is obtained via known models and reference, e.g. accelerometers and magnetometers, and 2) gyro sensors (either rate or rate-integrating type [3]). Accelerometers, gyros and optional magnetometers are commonly integrated into one package, namely, the inertial measurement units (IMUs), to provide combined measurements of body acceleration, angular rate and direction of Earth magnetic field, from which the attitude can be (fully) resolved. With the advent of micro-electro-mechanical system (MEMS) technology, IMUs can be manufactured into very small and cheap electronic chips, being vastly used in consumer electronics (e.g. smart phones, tablets, gaming systems) [4], imaging stabilization devices and micro aerial vehicles (MAVs) [5], etc. However, the MEMS IMU has inherent defects. For example, accelerometers are sensitive to vibrations and translational acceleration, and the commonly used MEMS rate gyros randomly drift over time (i.e. gyro bias), which, once integrated, results in accumulated errors.

To achieve precise attitude estimation, various methods have been proposed over decades. A non-linear complementary filter operating on $SO(3)$ was introduced by Mahony *et al* [6]. In this method, the estimation of attitude and gyro bias is corrected by the residual error between the attitude estimation and measurement. This algorithm is with cheap computation and easy implementation. But due to the pre-setting constant correction gains, the estimation is usually suboptimal. Another vastly used attitude estimation approach is the extended Kalman filter (EKF), which is the workhorse of real-time attitude estimation in many robotic applications such as simultaneous localization and mapping (SLAM) [7], visual odometry (VO) [8], visual inertial navigation system (VINS) [9], virtual reality (VR) /augmented reality (AR) [10], etc. EKF is a well known and generic state estimation method for nonlinear systems. It extends the Kalman filter, which was first derived for linear systems and proved to be a minimum variance state estimator, to nonlinear systems by first-order linearization. Schmidt and his collaborators in the Apollo program [11] first applied the EKF framework to attitude estimation based on kinematic model. Nevertheless, in cases of the highly nonlinear dynamics or poor priori estimation of the state, the EKF usually fails [12]. The multiplicative EKF (MEKF) [13]–[15] based on the attitude error state was proposed to diminish the influence of linearization on $SO(3)$ and to avoid the covariance matrix being singular. Furthermore, unscented Kalman filter (UKF) [16] was proved to have relatively superior accuracy when the initial estimation error is large, by exploiting the second or higher order of Taylor series expansion of the nonlinear system.

One major limitation of both standard EKF and UKF based attitude estimation methods is that they often assume the observation (attitude measurements, e.g. acceleration, magnetic field, etc.) noises are white noise, and usually fail for more complicated but practical observation noises such as colorful noise, narrow-band noise, etc. that are caused by vibrations and environmental factors. Taking these non-ideal noises into consideration, further studies have been done based on specific assumptions or models. Sebesta *et al* [17] and Sarkka *et al* [18] respectively illustrated methods of adaptively estimating the measurement covariance matrix and tuning the EKF innovation in presence of white measurement noise with time-varying covariance. Qian *et al* [19] assumed a multiplicative measurement noise with unknown external disturbances, which lie in a bounded domain. Accordingly, the minimization of the estimated covariance can, to some extent, be achieved by minimizing the upper bound of the estimated covariance. Kumar and Crassidis [20] considered a colored measurement noise. In this scenario, the authors first characterized the noise by a second order vibration model and then augmented this model into the standard EKF framework.

Precisely modeling the noise is usually problematic because the noise is susceptible to various time-varying factors such as

[1]Guozheng Lu is with the R&D Department, DaJiang Innovations Science and Technology Co., Ltd, Shenzhen, China gene.lu@dji.com

[2]Fu Zhang, the corresponding author, is with the Department of Mechanical Engineering, the University of Hong Kong, Hong Kong, China fuzhang@hku.hk

system features and hostile environments. In contrast, digital filters like the low-pass filter can effectively attenuate the noise over a wide frequency range, eliminating the need for accurate noise modeling. One drawback of using such filter is that it may introduce considerable delay in attitude estimation, which is one of the main causes of overshoot and even divergence in attitude feedback control. Lozano *et al* [21] and Sanz *et al* [22] proposed to compensate constant delays by a state predictor, which predicts the current state by delayed state measurement, previous control input and lag time. Although constant delays caused by data transfer or computation can be accurately captured, they can barely describe a digital filter (e.g. low-pass filter), whose delay nonlinearly depends on frequencies of input signals. In this paper, we regard the digital filter as a part of the system model, leading to an augmented attitude kinematic model. We then incorporate such filters into the state observer (e.g. MEKF) framework to eliminate the transient error caused by the filter. It is not hard to imagine that when both the state observer predicted output and the actual system output are filtered by the same filter, the resulting estimation error will remain synced and no transient error will be present. Accordingly, modeling a digital filter in the observer, instead of approximating to the complex noise, can be a more generic and robust solution.

The original motivation of this paper is to solve the IMU-based attitude estimation problem of multi-axis gimbal systems [2], which have been increasingly used in unmanned aerial vehicles (UAVs) for imaging stabilization. The gimbal system is susceptible to various vibrations, caused by structural modes of itself and the host aerial vehicle , as well as the propeller induced vibration. These vibrations are translational motions and will be picked up by accelerometers. Since a gimbal system uses the accelerometer measurements to determine its payload attitude, the picked up translational vibrations will behave as a noise and significantly degrade the attitude estimation accuracy. To address these vibrations, vibration absorbers made by particular mechanism or soft material, are usually used to isolate vibrations from the aircraft. Due to their frequency response, vibration absorbers can effectively suppress high frequency noises such as propeller vibration and certain flexible modes of the aircraft. However, as shown in Fig.1, a low frequency translation acceleration is commonly seen at high speed forward flight, possibly due to the unsteady aerodynamic turbulence being created on the gimbal system. Such a noise is characterized by its narrow bandwidth (e.g. several Hz) and concentration on very low frequency (e.g. under 10 Hz), that cannot be effectively attenuated by the vibration absorber.

In this work, we consider the IMU based attitude estimation in the presence of narrow-band noise. Our main contribution is an attitude estimation algorithm that can effectively attenuate narrow-band noise concentrating at a very low frequency range and with time-varying dominant frequency. The developed algorithm comprises three components: an augmented MEKF framework in discrete time domain, a notch filter that attenuates the narrow-band noise, and a least mean square based adaptive algorithm that accurately identifies the noise dominant frequency in real time [23]. Experiments on actual gimbal systems show that the developed algorithm can accurately track the noise dominant frequency and attenuate the narrow-band noise without inducing much delay in the attitude estimation. Although verified on gimbal systems, the proposed algorithms can also be applied to other robotic platforms (e.g. UAVs) for attitude estimation in the presence of narrow-band noise.

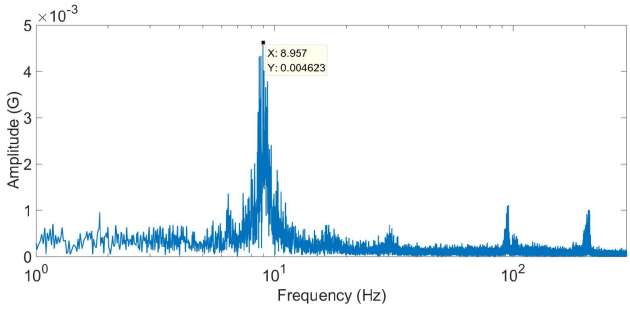

Fig. 1. Frequency spectrum of the accelerometer noise when the host aerial vehicle is flying at high speed.

This paper is organized as follows. Section II briefly introduces the attitude kinematics and the sensor models concerned in this paper. In section III, the standard MEKF framework is derived in discrete time domain. Section IV extends the standard MEKF to account for the dynamics of notch filter. With additional consideration on noise frequency drifting, adaptive frequency estimation method is adopted in section V. Section VI details the application to an inertially stabilized gimbal system and presents our experimental results to demonstrate the effectiveness of noise rejection and real-time attitude estimation. Finally, section VII arrives at our conclusion.

II. Attitude Kinematics and Sensor Models

A. Special Orthogonal Group $SO(3)$

Because a gimbal system only involves orientation, it is sufficient to consider the special orthogonal group $SO(3)$.

A rotation $\mathbf{R}$ can be interpreted as a rotation about an axis $\boldsymbol{\xi}$ of angle θ. The axis $\boldsymbol{\xi}$ and angle θ are related to the rotation matrix by an *exponential map* [24]:

$$\mathbf{R} \quad = \quad \exp(\boldsymbol{\theta}_\times) \tag{1}$$

where $\boldsymbol{\theta} = \theta\boldsymbol{\xi}$ and $\|\boldsymbol{\xi}\| = 1$. $\exp(A) = \sum_{n=0}^{\infty} \frac{A^n}{n!}$ is matrix exponential. The subscript operation $\boldsymbol{\theta}_\times$ takes the elements of $\boldsymbol{\theta}$ to form a skew-symmetric matrix as follows

$$\boldsymbol{\theta}_\times \triangleq \begin{bmatrix} 0 & -\boldsymbol{\theta}_3 & \boldsymbol{\theta}_2 \\ \boldsymbol{\theta}_3 & 0 & -\boldsymbol{\theta}_1 \\ -\boldsymbol{\theta}_2 & \boldsymbol{\theta}_1 & 0 \end{bmatrix} \tag{2}$$

The inverse map of $(\cdot)_\times$ is denoted as $(\cdot)_\vee$ such that

$$(\boldsymbol{\theta}_\times)_\vee = \boldsymbol{\theta}; \quad \forall \boldsymbol{\theta} \in \mathbb{R}^3 \tag{3}$$

In practice, Eq. (1) is computed by Rodrigue's formula

$$\exp\left(\theta\boldsymbol{\xi}_\times\right) = I + \boldsymbol{\xi}_\times \sin\theta + \boldsymbol{\xi}_\times^2(1 - \cos\theta) \tag{4}$$

The inverse of Eq. (1) is called *logarithmic map*

$$\log \mathbf{R} = \frac{\theta}{2\sin\theta}\left(\mathbf{R} - \mathbf{R}^T\right) \tag{5}$$

where $\theta = \cos^{-1}\left(\frac{tr(\mathbf{R})-1}{2}\right)$. The formula given by (5) is singular at $\theta = \pi$ (or equivalently $tr(\mathbf{R}) = -1$), which should therefore be excluded from $SO(3)$. $\boldsymbol{\theta}_\times = \log \mathbf{R} \in so(3)$ is called the *exponential coordinate* of $\mathbf{R}$.

The attitude is related to angular rate $\boldsymbol{\omega}$ by [24]

$$\dot{\mathbf{R}} = \mathbf{R}\boldsymbol{\omega}_\times \tag{6}$$

which implies that, if the rotation is about a fixed axis $\mathbf{b}$ ($\|\mathbf{b}\| = 1$) and the amount of rotation is $\alpha(t)$ at time t, then the instantaneous attitude is

$$\mathbf{R}(t) = \mathbf{R}(0)e^{\mathbf{b}_\times \alpha(t)} \tag{7}$$

The relation between angular rate $\boldsymbol{\omega}$ in (6) and the time derivative of the instantaneous exponential coordinate $\boldsymbol{\theta}$ of $\mathbf{R}$ in (1 is given as follows [25].

$$\boldsymbol{\omega} = \mathbf{M}(\boldsymbol{\theta})^T \dot{\boldsymbol{\theta}} \tag{8}$$

where

$$\mathbf{M}(\boldsymbol{\theta}) = I + \left(\frac{1-\cos\|\boldsymbol{\theta}\|}{\|\boldsymbol{\theta}\|}\right)\frac{\boldsymbol{\theta}_\times}{\|\boldsymbol{\theta}\|} + \left(1 - \frac{\sin\|\boldsymbol{\theta}\|}{\|\boldsymbol{\theta}\|}\right)\frac{\boldsymbol{\theta}_\times^2}{\|\boldsymbol{\theta}\|^2} \tag{9}$$

B. Sensor Models

The body frame is practically defined as the frame of the IMU enclosure, where the axis orientation of gyros and accelerometers is assumed to be calibrated and aligned. As a result, the measurement of gyros and accelerometers is immediately interpreted as that in the body frame.

The gyro is typically modeled as [26]

$$\boldsymbol{\omega}_{m_k} = \boldsymbol{\omega}_k + \mathbf{b}_k + \mathbf{n}_{r_k} \tag{10}$$

$$\mathbf{b}_k = \mathbf{b}_{k-1} + \mathbf{n}_{w_{k-1}}\Delta t \tag{11}$$

where Δt is the sampling time, $\boldsymbol{\omega}_{m_k}$ and $\boldsymbol{\omega}_k$ are respectively the measured and true angular rate at the k-th time step, $\mathbf{n}_r$ is the measurement noise and assumed to be Gaussian white with zero mean, and $\mathbf{b}$ denotes the random-walk gyro bias driven by another zero-mean Gaussian white noise $\mathbf{n}_w$. Combining (7), (10) and (11) yields the system state space model in discrete time domain

$$\mathbf{R}_k = \mathbf{R}_{k-1}\exp\left((\boldsymbol{\omega}_{k-1})_\times \Delta t\right) \tag{12a}$$

$$\boldsymbol{\omega}_{k-1} = \boldsymbol{\omega}_{m_{k-1}} - \mathbf{b}_{k-1} - \mathbf{n}_{r_{k-1}}$$

$$\mathbf{b}_k = \mathbf{b}_{k-1} + \mathbf{n}_{w_{k-1}}\Delta t \tag{12b}$$

Considering the vibration noise, the accelerometer noise model is no longer white. Instead, the measurement $\mathbf{a}_m$ is related to the gravity $\mathbf{g}$ and translational acceleration $\mathbf{a}_c$, both expressed in body frame, by [27]

$$\mathbf{g}_k = \mathbf{R}_k^T \mathbf{e}_3 \tag{13a}$$

$$\mathbf{a}_{m_k} = -\mathbf{g}_k + \mathbf{a}_{c_k} + \mathbf{d}_k + \mathbf{n}_{a_k} \tag{13b}$$

where $\mathbf{e}_3 = [0\ 0\ 1]^T$, $\mathbf{d}$ denotes the vibration noise and $\mathbf{n}_a$ is a zero-mean Gaussian white noise to capture the random measurement noise. (13) simply states the fact that the accelerometer measures all forces acted on the body but gravity. This agrees with two common facts: 1) a free falling accelerometer leads to zero measurements; and 2) a static accelerometer reads an acceleration that is opposite to gravity. Also note that the translational acceleration $\mathbf{a}_c$ can be compensated via methods like GPS-derived acceleration, thus can be omitted from (13b).

In our concerned application, the yaw angle of the gimbal payload is computed from the host UAV attitude and the forward kinematics [2]. Its measurement model takes the following form, which is essentially the formula for computing yaw angle in ZXY Euler angles from a rotation matrix.

$$\psi_k = -\arctan\frac{\mathbf{e}_1^T\mathbf{R}_k\mathbf{e}_2}{\mathbf{e}_2^T\mathbf{R}_k\mathbf{e}_2} \tag{14a}$$

$$\psi_{m_k} = \psi_k + n_{y_k} \tag{14b}$$

where $\mathbf{e}_1 = [1\ 0\ 0]^T$ and $\mathbf{e}_2 = [0\ 1\ 0]^T$, ψ and ψ_m are respectively the true and measured yaw angle, n_y is the measurement noise caused by host vehicle attitude measurements and gimbal joint measurements. In cases where magnetometer is used, the measurement model will take a similar form as that of accelerometer in (13).

III. MULTIPLICATIVE EXTENDED KALMAN FILTER IN DISCRETE TIME DOMAIN

The kinematic model (12) is problematic for the use of extended Kalman filter, due to the orthogonality constraint on the rotation matrix $\mathbf{R}$. This leads to singularity issues when propagating the corresponding covariance matrix [13] on the kinematic model (12). To overcome this, [14] and [15] proposed to project the state error into an unconstrained space according to the linear relationship between the state representation and its corresponding error representation, instead of propagating the estimated state vector (i.e. the rotation matrix or quaternion which are constrained) directly. Then it propagates the covariance matrix and update a-posteriori state estimate using its error kinematic model (see (19)). To ease the following description, we call the original kinematic model defined in (12) as the "primal system" and the error kinematic model (see (19)) as the "error state system". Since the linear relationship between the primal state representation and error state representation implies a multiplication on the rotation matrix or quaternion, the resulting extended Kalman filter (EKF) is called a multiplicative EKF (MEKF) [14], [15]. The multiplicative EKF usually requires the state (e.g. attitude) estimate error to be very small, such that the error state system can well approximate the primal system. In practice, this requirement is usually met well for IMU based attitude estimation.

The original MEKF derivation in [13]–[15] are based on quaternion representation in continuous time domain. The derived MEKF is then discretized for actual implementation. In this paper, we derive the multiplicative EKF directly on $SO(3)$ in the discrete time domain (12), and subsequently extend it to the case with narrow-band noise.

A. Propagation of The Primal System

To start with, let us be at present time step k, with the a-posteriori state estimate at previous step $\hat{\mathbf{R}}_{k-1|k-1}$ and

$\widehat{\mathbf{b}}_{k-1|k-1}$. The goal of the EKF is to obtain the a-priori estimate and the a-posteriori estimate at the present time step.

The a-priori estimate can be immediately obtained from the state equation (12) by following the EKF, i.e.,

$$\widehat{\mathbf{R}}_{k|k-1} = \widehat{\mathbf{R}}_{k-1|k-1} \exp\left((\widehat{\boldsymbol{\omega}}_{k-1|k-1})_\times \Delta t\right) \tag{15a}$$

$$\widehat{\boldsymbol{\omega}}_{k-1|k-1} = \boldsymbol{\omega}_{m_{k-1}} - \widehat{\mathbf{b}}_{k-1|k-1} \tag{15b}$$

$$\widehat{\mathbf{b}}_{k|k-1} = \widehat{\mathbf{b}}_{k-1|k-1} \tag{15c}$$

B. Propagation of The Error State System

Since the state $\mathbf{R}$ is on a nonlinear differential manifold $SO(3)$, directly applying the EKF on the state $\mathbf{R}$ will cause singularity in the convariace propagation. To avoid this, we employ the attitude error representations over time steps $\tau \geq k-1$ as below

$$\delta\mathbf{R}_\tau \triangleq \widehat{\mathbf{R}}_{\tau|k-1}^T \mathbf{R}_\tau \tag{16a}$$

$$\Delta\mathbf{b}_\tau \triangleq \mathbf{b}_\tau - \widehat{\mathbf{b}}_{\tau|k-1} \tag{16b}$$

where $\widehat{\mathbf{R}}_{\tau|k-1}$ is the attitude prediction at step τ based on all outputs up to the previous time step $k-1$, and is updated by the following state equation

$$\widehat{\mathbf{R}}_{\tau|k-1} = \widehat{\mathbf{R}}_{\tau-1|k-1} \exp\left((\widehat{\boldsymbol{\omega}}_{\tau-1|k-1})_\times \Delta t\right) \tag{17a}$$

$$\widehat{\boldsymbol{\omega}}_{\tau-1|k-1} = \boldsymbol{\omega}_{m_{\tau-1}} - \widehat{b}_{\tau-1|k-1}$$

$$\widehat{\mathbf{b}}_{\tau|k-1} = \widehat{\mathbf{b}}_{\tau-1|k-1} \tag{17b}$$

for $\tau \geq k$. From the definition in (16), one can easily obtain

$$\delta\widehat{\mathbf{R}}_{k-1|k-1} = \widehat{\mathbf{R}}_{k-1|k-1}^T \widehat{\mathbf{R}}_{k-1|k-1} = \mathbf{I}_{3\times3} \tag{18a}$$

$$\Delta\widehat{\mathbf{b}}_{k-1|k-1} = \widehat{\mathbf{b}}_{k-1|k-1} - \widehat{\mathbf{b}}_{k-1|k-1} = \mathbf{0}_{3\times1} \tag{18b}$$

The key idea of MEKF is that it estimates the error state (i.e. $\delta\mathbf{R}$ and $\Delta\mathbf{b}$) instead of the original system state (i.e. $\mathbf{R}$ and $\mathbf{b}$). To do so, the state equation of the error state is required. Substituting the state equation of ground truth system (12) and the predicted system (17) into error state system (16) leads to

$$\delta\mathbf{R}_\tau = \exp\left(-(\widehat{\boldsymbol{\omega}}_{\tau-1|k-1})_\times \Delta t\right) \delta\mathbf{R}_{\tau-1} \exp\left((\boldsymbol{\omega}_{\tau-1})_\times \Delta t\right) \tag{19a}$$

$$\Delta\mathbf{b}_\tau = \Delta\mathbf{b}_{\tau-1} + \mathbf{n}_{w_{\tau-1}} \Delta t \tag{19b}$$

Let $\delta\theta$, $\boldsymbol{\xi}$ and $\delta\boldsymbol{\theta}$ be respectively the rotation angle, rotation axis and axis-angle associated with the error attitude $\delta\mathbf{R}$ such that $\delta\boldsymbol{\theta} = \delta\theta \cdot \boldsymbol{\xi}$ and $\delta\mathbf{R} = \exp\left((\delta\boldsymbol{\theta})_\times\right)$, then (19a) can be rewritten as

$$\exp\left((\delta\boldsymbol{\theta}_\tau)_\times\right) = \exp\left(-(\widehat{\boldsymbol{\omega}}_{\tau-1|k-1})_\times \Delta t\right) \exp\left((\delta\boldsymbol{\theta}_{\tau-1})_\times\right) \exp\left((\widehat{\boldsymbol{\omega}}_{\tau-1|k-1} - \Delta\mathbf{b}_{\tau-1} - \mathbf{n}_{r_{\tau-1}})_\times \Delta t\right) \tag{20}$$

Equation (20) is the exact nonlinear error state equation. This extremely nonlinear state equation can be linearized by assuming the error state being small, which leads to the axis-angle presentation

$$\delta\mathbf{R} = \exp\left(\delta\boldsymbol{\theta}_\times\right) \approx \mathbf{I}_{3\times3} + (\delta\boldsymbol{\theta})_\times \tag{21}$$

Substituting (21) into (20) and neglecting higher order terms yields the linearized error state equation as follows:

$$\begin{bmatrix} \delta\boldsymbol{\theta}_\tau \\ \Delta\mathbf{b}_\tau \end{bmatrix} = \begin{bmatrix} \exp\left(-(\widehat{\boldsymbol{\omega}}_{\tau-1|k-1}\Delta t)_\times\right) & -\mathbf{M}(\widehat{\boldsymbol{\omega}}_{\tau-1|k-1}\Delta t)\Delta t \\ \mathbf{0}_{3\times3} & \mathbf{I}_{3\times3} \end{bmatrix} \cdot \begin{bmatrix} \delta\boldsymbol{\theta}_{\tau-1} \\ \Delta\mathbf{b}_{\tau-1} \end{bmatrix} + \begin{bmatrix} -\mathbf{M}(\widehat{\boldsymbol{\omega}}_{\tau-1|k-1}\Delta t)\Delta t & \mathbf{0}_{3\times3} \\ \mathbf{0}_{3\times3} & \mathbf{I}_{3\times3}\Delta t \end{bmatrix} \begin{bmatrix} \mathbf{n}_{r_{\tau-1}} \\ \mathbf{n}_{w_{\tau-1}} \end{bmatrix} \tag{22}$$

where $\mathbf{w}(\tau-1) \sim \mathcal{N}(\mathbf{0}, \mathcal{Q}(\tau-1))$, $\tau \geq k$, meaning that the error system starts from the previous time step $k-1$, and $\mathbf{M}(\cdot)$ takes the definitions of (9). For MEMS gyros concerned in this paper, the sampling rate is quite high (e.g. up to several kHz), second order terms $(\Delta t)^2$ can be safely neglected, which leads to $\mathbf{M}(\widehat{\boldsymbol{\omega}}_{\tau-1|k-1}\Delta t)\Delta t \approx \mathbf{I}_{3\times3}\Delta t$. In practice, the linearized error system in (22) can be simplified as

$$\underbrace{\begin{bmatrix} \delta\boldsymbol{\theta}_\tau \\ \Delta\mathbf{b}_\tau \end{bmatrix}}_{\mathbf{X}_\tau} = \underbrace{\begin{bmatrix} \exp\left(-(\widehat{\boldsymbol{\omega}}_{\tau-1|k-1}\Delta t)_\times\right) & -\mathbf{I}_{3\times3}\Delta t \\ \mathbf{0}_{3\times3} & \mathbf{I}_{3\times3} \end{bmatrix}}_{\mathbf{F}_{\tau-1}} \underbrace{\begin{bmatrix} \delta\boldsymbol{\theta}_{\tau-1} \\ \Delta\mathbf{b}_{\tau-1} \end{bmatrix}}_{\mathbf{X}_{\tau-1}} + \underbrace{\begin{bmatrix} -\mathbf{I}_{3\times3}\Delta t & \mathbf{0}_{3\times3} \\ \mathbf{0}_{3\times3} & \mathbf{I}_{3\times3}\Delta t \end{bmatrix}}_{\mathbf{B}_w} \underbrace{\begin{bmatrix} \mathbf{n}_{r_{\tau-1}} \\ \mathbf{n}_{w_{\tau-1}} \end{bmatrix}}_{\mathbf{w}_{\tau-1}} \tag{23}$$

The multiplicative extended Kalman filter propagates the error state and the associated covariance matrix by the linearized state equation (23) instead of the original system equation (12). When the attitude measurements are received at a lower rate than that of the gyro, there are multiple gyro measurements in between two consecutive attitude measurements. In this case, as the error system (23) is defined over all time steps $\tau \geq k-1$, it enables the state and covariance matrix to keep propagating from previous measurement at time step $k-1$ until the next measurement is received.

Without loss of generality, we assume the attitude measurement is at the same rate of gyro. That is, the attitude measurement is received at each gyro sample. In this case, we would only be required to propagate the state and covariance matrix by one step forward (i.e. to step k), where new attitude measurement is received and used to update the propagated state estimate. Applying the standard Kalman filter procedure to (23), which is a time varying linear system, we have the error state and covariance matrix propagation,which are respectively denoted as $\widehat{\mathbf{X}}_{k|k-1}$ and $\mathbf{P}_{k|k-1}$, as follows:

$$\widehat{\mathbf{X}}_{k|k-1} = \mathbf{F}_{k-1}\widehat{\mathbf{X}}_{k-1|k-1} = \mathbf{0}_{6\times1} \tag{24a}$$

$$\mathbf{P}_{k|k-1} = \mathbf{F}_{k-1}\mathbf{P}_{k-1|k-1}\mathbf{F}_{k-1}^T + \mathbf{B}_w\mathcal{Q}_{k-1}\mathbf{B}_w^T \tag{24b}$$

where $\widehat{\mathbf{X}}_{k-1|k-1}$ and $\mathbf{P}_{k-1|k-1}$ are respectively the a-posteriori estimate of the error state and the covariance matrix of the estimate. We have $\widehat{\mathbf{X}}_{k-1|k-1} = \mathbf{0}_{6\times1}$ as a result of (18).

C. Update of The Error State System

Next, to derive the output equation, the standard EKF assumes that the attitude $\mathbf{R}$ is obtainable at the rate of system measurements, either by the combination of an accelerometer and a magnetometer or by other means (e.g. visual sensors). Denote $\mathbf{R}_m$ be the attitude measurement, $\mathbf{R}_m$ is generally modeled as

$$\mathbf{R}_m = \mathbf{R}\mathbf{R}_n \tag{25}$$

where $\mathbf{R}_n$ is the measurement noise, which is very small and assumed as $\mathbf{R}_n = \exp(\mathbf{v}_\times)$, where $\mathbf{v} \sim \mathcal{N}(\mathbf{0}, \mathcal{R})$ is the axis-angle representation of the measurement noise $\mathbf{R}_n$.

The output in the standard EKF, at the time step k, is then defined as exponential coordinate of the error attitude between the measurement and the most recent estimate (i.e. the a-priori estimate)

$$\mathbf{Z}_k = \left(\log\left(\widehat{\mathbf{R}}_{k|k-1}^T \mathbf{R}_{m_k}\right)\right)_\vee \tag{26}$$

where $\log(\cdot)$ is the matrix logarithm map.

Substituting (16a) and (25) into (26) and neglecting higher order terms such as $\delta\boldsymbol{\theta}_k \times \mathbf{v}_k$, we obtain the output equation as below

$$\mathbf{Z}_k = \underbrace{\begin{bmatrix}\mathbf{I}_{3\times3} & \mathbf{0}_{3\times3}\end{bmatrix}}_{\mathbf{H}_k}\begin{bmatrix}\delta\boldsymbol{\theta}_k \\ \Delta\mathbf{b}_k\end{bmatrix} + \mathbf{v}_k \tag{27}$$

Recalling (24) and following the standard Kalman filter procedure, we obtain the update of the error state system as below

$$\mathbf{S}_k = \mathbf{H}_k\mathbf{P}_{k|k-1}\mathbf{H}_k^T + \mathcal{R}_k \tag{28a}$$
$$\mathbf{K}_k = \mathbf{P}_{k|k-1}\mathbf{H}_k^T\mathbf{S}_k^{-1} \tag{28b}$$
$$\widehat{\mathbf{X}}_{k|k} = \mathbf{K}_k\mathbf{Z}_k \tag{28c}$$
$$\mathbf{P}_{k|k} = (\mathbf{I}_{6\times6} - \mathbf{K}_k\mathbf{H}_k)\mathbf{P}_{k|k-1} \tag{28d}$$

Therefore, we have

$$\delta\widehat{\boldsymbol{\theta}}_{k|k} = \mathbf{E}_1\mathbf{K}_k\mathbf{Z}_k \tag{29a}$$
$$\Delta\widehat{\mathbf{b}}_{k|k} = \mathbf{E}_2\mathbf{K}_k\mathbf{Z}_k \tag{29b}$$

where $\mathbf{E}_1 = [\mathbf{I}_{3\times3}\ \mathbf{0}_{3\times3}]$ and $\mathbf{E}_1 = [\mathbf{0}_{3\times3}\ \mathbf{I}_{3\times3}]$.

D. Update of The Primal System

After obtaining the prediction and update of the error state system respectively given in (24) and (28), the next is to derive the update step of the primal system (i.e. attitude and gyro bias). Again, recalling the definition in (16), we have

$$\mathbf{R}_k = \widehat{\mathbf{R}}_{k|k-1}\delta\mathbf{R}_k \tag{30a}$$
$$\mathbf{b}_k = \widehat{\mathbf{b}}_{k|k-1} + \Delta\mathbf{b}_k \tag{30b}$$

which leads to the estimate respectively shown as below

$$\widehat{\mathbf{R}}_{k|k} = \widehat{\mathbf{R}}_{k|k-1}\delta\widehat{\mathbf{R}}_{k|k} \tag{31a}$$
$$\widehat{\mathbf{b}}_{k|k} = \widehat{\mathbf{b}}_{k|k-1} + \Delta\widehat{\mathbf{b}}_{k|k} \tag{31b}$$

Substituting (29) into the above equation yields

$$\widehat{\mathbf{R}}_{k|k} = \widehat{\mathbf{R}}_{k|k-1}\exp\left((\mathbf{E}_1\mathbf{K}_k\mathbf{Z}_k)_\times\right) \tag{32a}$$
$$\widehat{\mathbf{b}}_{k|k} = \widehat{\mathbf{b}}_{k|k-1} + \mathbf{E}_2\mathbf{K}_k\mathbf{Z}_k \tag{32b}$$

E. The multiplicative EKF Algorithm on $SO(3)$

Finally, the complete multiplicative extended Kalman filter on $SO(3)$ can be summarized in **Algorithm. 1**.

Algorithm 1 Multiplicative EKF algorithm on $SO(3)$

Initialization: $\widehat{\mathbf{R}}_{0|-1} = \mathbf{E}[\mathbf{R}_0]$; $\widehat{\mathbf{b}}_{0|-1} = \mathbf{b}_0; \mathbf{P}_{0|-1} = \mathbf{P}_0$

for k = 0, 1, 2, ... ,N **do**

Update:

$\mathbf{Z}_k = \left(\log\left(\widehat{\mathbf{R}}_{k|k-1}^T\mathbf{R}_{m_k}\right)\right)_\vee$

$\mathbf{S}_k = \mathbf{H}_k\mathbf{P}_{k|k-1}\mathbf{H}_k^T + \mathcal{R}_k$

$\mathbf{K}_k = \mathbf{P}_{k|k-1}\mathbf{H}_k^T\mathbf{S}_k^{-1}$

$\widehat{\mathbf{R}}_{k|k} = \widehat{\mathbf{R}}_{k|k-1}\exp\left((\mathbf{E}_1\mathbf{K}_k\mathbf{Z}_k)_\times\right)$

$\widehat{\mathbf{b}}_{k|k} = \widehat{\mathbf{b}}_{k|k-1} + \mathbf{E}_2\mathbf{K}_k\mathbf{Z}_k$

$\mathbf{P}_{k|k} = (\mathbf{I}_{6\times6} - \mathbf{K}_k\mathbf{H}_k)\mathbf{P}_{k|k-1}$

Predict:

$\widehat{\boldsymbol{\omega}}_{k|k} = \boldsymbol{\omega}_{m_k} - \widehat{\mathbf{b}}_{k|k}$

$\widehat{\mathbf{R}}_{k+1|k} = \widehat{\mathbf{R}}_{k|k}\exp\left((\widehat{\boldsymbol{\omega}}_{k|k})_\times\Delta t\right)$

$\widehat{\mathbf{b}}_{k+1|k} = \widehat{\mathbf{b}}_{k|k}$

$\mathbf{P}_{k+1|k} = \mathbf{F}_k\mathbf{P}_{k|k}\mathbf{F}_k^T + \mathbf{B}_w\mathcal{Q}_k\mathbf{B}_w^T$

end for

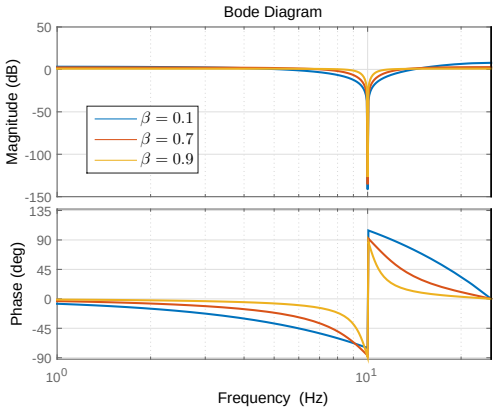

Fig. 2. Bode diagram of notch filters with $\omega_0 = 10Hz$, $\alpha = 1.0$ and different values of β, the sampling frequency is $50Hz$ (i.e. $\Delta t = 0.02$ sec)

IV. Augmented MEKF with The Notch Filter

As mentioned in the introduction, the translational vibration considerably contaminates the accelerometer measurement, usually leading to poor attitude estimation based on the multiplicative EKF algorithm presented previously. Since the frequency range of such noise is narrow, we apply a notch filter to attenuate the vibration noise. The transfer function of a notch filter in discrete time domain is represented as

$$G_f(z) = \frac{z^2 - 2\alpha\cos(\omega_0\Delta t)z + \alpha^2}{z^2 - 2\beta\cos(\omega_0\Delta t)z + \beta^2} \tag{33}$$

where z is the $\mathcal{Z}$-transform variable, Δt is the sampling time as before, ω_0 is the dominant noise frequency, α and β are damping ratio-like parameters that are used to tune the depth and width of the notch filter. In practice, we usually set $\alpha = 1$ for large attenuation at the notch frequency ω_0 and use β to tune the width of the notch. Fig. 2 shows the Bode plot of notch filters with $\omega_0 = 10Hz$, $\alpha = 1$ and different values of β. It is seen that a smaller β results in a wider attenuation around the notch frequency but with the drawback of amplifying noise at high frequency range. When $\beta = 0.7$, notch filter achieves around 150dB (i.e. $10^{-7.5}$) attenuation at the frequency ω_0 without considerably amplifying noise in other frequencies.

The employed notch filter can be explicitly represented by a linear state space model, known as state space realization [28]

$$\begin{aligned}\mathbf{x}_{f_k} &= \mathbf{A}\mathbf{x}_{f_{k-1}} + \mathbf{B}\left(\mathbf{a}_{m_{k-1}} - \mathbf{a}_{c_{k-1}}\right)\\ \mathbf{a}_{f_k} &= \mathbf{C}\mathbf{x}_{f_k} + \mathbf{D}\left(\mathbf{a}_{m_k} - \mathbf{a}_{c_k}\right)\end{aligned} \tag{34}$$

where $\mathbf{x}_f$ is the state of the notch filter, $\mathbf{a}_{m_k} - \mathbf{a}_{c_k}$ is the accelerometer raw measurements compensated by translational acceleration, and $\mathbf{a}_{f_k}$ is the filtered accelerometer readings, which will be fed into the MEKF for attitude and bias estimation. Assume M notch filters are used for each channel to achieve the required level of noise attenuation, the filter for each channel is order of $N = 2M$, and $\mathbf{A} = \text{diag}(\mathbf{A}_1\ \mathbf{A}_2\ \mathbf{A}_3) \in \mathbb{R}^{3N\times3N}$; $\mathbf{B} = \text{diag}(\mathbf{B}_1\ \mathbf{B}_2\ \mathbf{B}_3) \in \mathbb{R}^{3N\times3}$; $\mathbf{C} = \text{diag}(\mathbf{C}_1\ \mathbf{C}_2\ \mathbf{C}_3) \in \mathbb{R}^{3\times3N}$ and $\mathbf{D} = \text{diag}(\mathbf{D}_1\ \mathbf{D}_2\ \mathbf{D}_3) \in \mathbb{R}^{3\times3}$. The group of $\mathbf{A}_i, \mathbf{B}_i, \mathbf{C}_i$ and $\mathbf{D}_i$ is the state space representation of (33) for each channel. When only one notch filter is used for the channel, one possible group of $\mathbf{A}_i, \mathbf{B}_i, \mathbf{C}_i$ and $\mathbf{D}_i$ are as follows (i.e. the controllable canonical realization [28]).

$$\mathbf{A}_i = \begin{bmatrix}0 & 1\\ -\beta^2 & 2\beta\cos(\omega_0\Delta t)\end{bmatrix}, \quad \mathbf{B}_i = \begin{bmatrix}0\\1\end{bmatrix}, \tag{35a}$$
$$\mathbf{C}_i = \begin{bmatrix}\alpha^2 - \beta^2 & 2(\beta - \alpha)\cos(\omega_0\Delta t)\end{bmatrix}, \quad \mathbf{D}_i = 1 \tag{35b}$$

Shown in Fig. 2, due to the large attenuation around the notch frequency ω_0, which is the dominant frequency components of the narrow-band noise, the filtered accelerometer measurements will be susceptible to no such vibration noise. However, Fig. 2 shows that the

added notch filter introduces significant phase lag to the input signal, which in turn potentially leads to overshoot or even divergence in attitude control.

To eliminate the delay, we regard the added notch filter as a part of the original system and form an augmented system model. We then explicitly incorporate the notch filter dynamics in the state observer. In the case of linear system, the augmented system will remain observable and the resulting Kalman filter will therefore converge to ground truth state [28]. Furthermore, due to the large attenuation of the notch filter, the narrow-band vibration noise shows no effect on the filter output and can be removed from the accelerometer model in (13b). As a result, the augmented system can be written as

$$\mathbf{R}_k = \mathbf{R}_{k-1}\exp\left((\boldsymbol{\omega}_{k-1})_\times \Delta t\right) \tag{36a}$$
$$\boldsymbol{\omega}_{k-1} = \boldsymbol{\omega}_{m_{k-1}} - \mathbf{b}_{k-1} - \mathbf{n}_{r_{k-1}}$$
$$\mathbf{b}_k = \mathbf{b}_{k-1} + \mathbf{n}_{w_{k-1}}\Delta t \tag{36b}$$
$$\mathbf{x}_{f_k} = \mathbf{A}\mathbf{x}_{f_{k-1}} + \mathbf{B}\left(\mathbf{a}_{m_{k-1}} - \mathbf{a}_{c_{k-1}}\right) \tag{36c}$$
$$\mathbf{a}_{m_{k-1}} = -\mathbf{g}_{k-1} + \mathbf{a}_{c_{k-1}} + \mathbf{n}_{a_{k-1}}$$

To linearize the augmented system similar to the standard EKF case, we predict the augmented states based on all the outputs up to $k-1$ by the following system

$$\widehat{\mathbf{x}}_{f_{\tau|k-1}} = \mathbf{A}\widehat{\mathbf{x}}_{f_{\tau-1|k-1}} - \mathbf{B}\widehat{\mathbf{R}}^T_{\tau-1|k-1}\mathbf{e}_3; \quad \tau \geq k \tag{37}$$

The prediction of attitude and gyro bias is identical to (17).

Following the standard EKF case, we define the error filter state $\Delta\mathbf{x}_f$ as the deviation between the predicted filter state $\widehat{\mathbf{x}}_{f_{\tau|k-1}}$ and its true value $\mathbf{x}_{f_\tau}$

$$\Delta\mathbf{x}_{f_\tau} = \mathbf{x}_{f_\tau} - \widehat{\mathbf{x}}_{f_{\tau|k-1}} \tag{38}$$

Substituting (36c), (37) and (16) into (38), one can obtain

$$\Delta\mathbf{x}_{f_\tau} = \mathbf{A}\Delta\mathbf{x}_{f_{\tau-1}} - \mathbf{B}\left(\widehat{\mathbf{R}}^T_{\tau-1|k-1}\mathbf{e}_3\right)_\times \delta\boldsymbol{\theta}_{\tau-1} + \mathbf{B}\mathbf{n}_{a_{\tau-1}} \tag{39}$$

Therefore, the augmented system represented by its error state can be written as

$$\underbrace{\begin{bmatrix}\delta\boldsymbol{\theta}_\tau\\ \Delta\mathbf{b}_\tau\\ \Delta\mathbf{x}_{f_\tau}\end{bmatrix}}_{\overline{\mathbf{X}}(\tau)} = \underbrace{\begin{bmatrix}\exp\left(-(\widehat{\boldsymbol{\omega}}_{\tau-1|k-1})_\times\Delta t\right) & -\mathbf{I}_{3\times3}\Delta t & \mathbf{0}_{3\times3N}\\ \mathbf{0}_{3\times3} & \mathbf{I}_{3\times3} & \mathbf{0}_{3\times3N}\\ -\mathbf{B}\left(\widehat{\mathbf{R}}^T_{\tau-1|k-1}\mathbf{e}_3\right)_\times & \mathbf{0}_{3N\times3} & \mathbf{A}\end{bmatrix}}_{\overline{\mathbf{F}}_{\tau-1}} \cdot \underbrace{\begin{bmatrix}\delta\boldsymbol{\theta}_{\tau-1}\\ \Delta\mathbf{b}_{\tau-1}\\ \Delta\mathbf{x}_{f_{\tau-1}}\end{bmatrix}}_{\overline{\mathbf{X}}_{\tau-1}} + \underbrace{\begin{bmatrix}-\mathbf{I}_{3\times3}\Delta t & \mathbf{0}_{3\times3} & \mathbf{0}_{3\times3}\\ \mathbf{0}_{3\times3} & \mathbf{I}_{3\times3}\Delta t & \mathbf{0}_{3\times3}\\ \mathbf{0}_{3N\times3} & \mathbf{0}_{3N\times3} & \mathbf{B}\end{bmatrix}}_{\overline{\mathbf{B}}_w}\underbrace{\begin{bmatrix}\mathbf{n}_{r_{\tau-1}}\\ \mathbf{n}_{w_{\tau-1}}\\ \mathbf{n}_{a_{\tau-1}}\end{bmatrix}}_{\overline{\mathbf{w}}_{\tau-1}} \tag{40}$$

where $\overline{\mathbf{w}}(\tau-1) \sim \mathcal{N}(\mathbf{0}, \overline{\mathcal{Q}}(\tau-1))$, and $\tau \geq k$.

Implied by (38), we have $\Delta\mathbf{x}_{f_{k-1|k-1}} = \mathbf{x}_{f_{k-1|k-1}} - \mathbf{x}_{f_{k-1|k-1}} = \mathbf{0}_{3N\times1}$ and $\widehat{\overline{\mathbf{X}}}_{k-1|k-1} = \mathbf{0}_{(3N+6)\times1}$. Similar to the standard EKF case, we assume the attitude measurement is at the same rate of gyro and would be only required to propagate for one step forward:

$$\widehat{\overline{\mathbf{X}}}_{k|k-1} = \overline{\mathbf{F}}_{k-1}\widehat{\overline{\mathbf{X}}}_{k-1|k-1} = \mathbf{0}_{(3N+6)\times1} \tag{41a}$$
$$\overline{\mathbf{P}}_{k|k-1} = \overline{\mathbf{F}}_{k-1}\overline{\mathbf{P}}_{k-1|k-1}\overline{\mathbf{F}}^T_{k-1} + \overline{\mathbf{B}}_w\overline{\mathcal{Q}}_{k-1}\overline{\mathbf{B}}^T_w \tag{41b}$$

Next, the measurements of the augmented system are the filtered accelerometer signal and the yaw measurement, i.e,

$$\mathbf{a}_{f_k} = \mathbf{C}\mathbf{x}_{f_k} + \mathbf{D}\left(\mathbf{a}_{m_k} - \mathbf{a}_{c_k}\right) \tag{42a}$$
$$\psi_{m_k} = \psi_k + n_{y_k} \tag{42b}$$

The output of the augmented system is then defined as

$$\overline{\mathbf{Z}}_k = \begin{bmatrix}\mathbf{a}_{f_k} - \widehat{\mathbf{a}}_{f_{k|k-1}}\\ \psi_{m_k} - \widehat{\psi}_{k|k-1}\end{bmatrix}; \quad \tau \geq k \tag{43}$$

where $\widehat{\mathbf{a}}_f$ and $\widehat{\psi}$ are respectively the predicted filter output and the predicted yaw angle, i.e.,

$$\widehat{\mathbf{a}}_{f_{k|k-1}} = \mathbf{C}\widehat{\mathbf{x}}_{f_{k|k-1}} - \mathbf{D}\widehat{\mathbf{R}}^T_{k|k-1}\mathbf{e}_3 \tag{44a}$$
$$\widehat{\psi}_{k|k-1} = -\arctan\frac{\mathbf{e}_1^T\widehat{\mathbf{R}}_{k|k-1}\mathbf{e}_2}{\mathbf{e}_2^T\widehat{\mathbf{R}}_{k|k-1}\mathbf{e}_2} \tag{44b}$$

Substituting (42) and (44) into (43) produces

$$\overline{\mathbf{Z}}_k = \underbrace{\begin{bmatrix}-\mathbf{D}\left(\widehat{\mathbf{R}}^T_{k|k-1}\mathbf{e}_3\right)_\times & \mathbf{0}_{3\times3} & \mathbf{C}\\ \mathbf{H}_{f_k} & \mathbf{0}_{1\times3} & \mathbf{0}_{1\times3N}\end{bmatrix}}_{\overline{\mathbf{H}}_k}\underbrace{\begin{bmatrix}\delta\boldsymbol{\theta}_k\\ \Delta\mathbf{b}_k\\ \Delta\mathbf{x}_{f_k}\end{bmatrix}}_{\overline{\mathbf{X}}_k} + \underbrace{\begin{bmatrix}\mathbf{D} & \mathbf{0}_{3\times1}\\ 0 & 1\end{bmatrix}}_{\overline{\mathbf{D}}_v}\underbrace{\begin{bmatrix}\mathbf{n}_{a_k}\\ n_{y_k}\end{bmatrix}}_{\overline{\mathbf{v}}_k} \tag{45}$$

where $\overline{\mathbf{v}}_k \sim \mathcal{N}(\mathbf{0}, \overline{\mathcal{R}}_k)$ and

$$\mathbf{H}_f = \begin{bmatrix}\frac{\widehat{r}_{23}\widehat{r}_{12}-\widehat{r}_{13}\widehat{r}_{22}}{\widehat{r}^2_{12}+\widehat{r}^2_{22}} & 0 & \frac{\widehat{r}_{11}\widehat{r}_{22}-\widehat{r}_{21}\widehat{r}_{12}}{\widehat{r}^2_{12}+\widehat{r}^2_{22}}\end{bmatrix} \tag{46}$$

$\widehat{r}_{ij}$ is the i-th row j-th column element of matrix $\widehat{\mathbf{R}}_{k|k-1}$.

Similar to the standard multiplicative EKF case, recalling (41) and following the standard Kalman filter procedure, we obtain the update of the augmented error state system

$$\overline{\mathbf{S}}_k = \overline{\mathbf{H}}_k\overline{\mathbf{P}}_{k|k-1}\overline{\mathbf{H}}^T_k + \overline{\mathbf{D}}_v\overline{\mathcal{R}}_k\overline{\mathbf{D}}^T_v \tag{47a}$$
$$\overline{\mathbf{K}}_k = \overline{\mathbf{P}}_{k|k-1}\overline{\mathbf{H}}^T_k\overline{\mathbf{S}}^{-1}_k \tag{47b}$$
$$\widehat{\overline{\mathbf{X}}}_{k|k} = \overline{\mathbf{K}}_k\overline{\mathbf{Z}}_k \tag{47c}$$
$$\overline{\mathbf{P}}_{k|k} = (\mathbf{I}_{(3N+6)\times(3N+6)} - \overline{\mathbf{K}}_k\overline{\mathbf{H}}_k)\overline{\mathbf{P}}_{k|k-1} \tag{47d}$$

Therefore, we have

$$\delta\widehat{\boldsymbol{\theta}}_{k|k} = \overline{\mathbf{E}}_1\overline{\mathbf{K}}_k\overline{\mathbf{Z}}_k \tag{48a}$$
$$\Delta\widehat{\mathbf{b}}_{k|k} = \overline{\mathbf{E}}_2\overline{\mathbf{K}}_k\overline{\mathbf{Z}}_k \tag{48b}$$
$$\Delta\widehat{\mathbf{x}}_{f_{k|k}} = \overline{\mathbf{E}}_3\overline{\mathbf{K}}_k\overline{\mathbf{Z}}_k \tag{48c}$$

where $\overline{\mathbf{E}}_1 = [\mathbf{I}_{3\times3}\ \mathbf{0}_{3\times3}\ \mathbf{0}_{3\times3N}]$, $\overline{\mathbf{E}}_2 = [\mathbf{0}_{3\times3}\ \mathbf{I}_{3\times3}\ \mathbf{0}_{3\times3N}]$ and $\overline{\mathbf{E}}_3 = [\mathbf{0}_{3N\times3}\ \ \mathbf{0}_{3N\times3}\ \ \mathbf{I}_{3N\times3N}]$.

Finally, the complete multiplicative extended Kalman filter with a notch filter can be summarized in **Algorithm. 2**.

V. Adaptive Noise Frequency Estimation

As the dominant noise frequency usually drifts over time or over the environment, it is necessary to identify the noise frequency in real time and tune the notch frequency accordingly. We adopt the adaptive frequency estimation (AFE) scheme proposed by Jia in [23]. Assume the noise dominant frequency is ω_0, then the vibration noise d can be written as

$$d_k = A\sin(\omega_0 k\Delta t + \varphi) \tag{49}$$

where A, φ are respectively the amplitude and phase of the dominant noise.

Using the parameterization in (49), we can prove that the following relation holds

$$d_k - \eta d_{k-1} + d_{k-2} = 0 \tag{50}$$

where $\eta = 2\cos(\omega_0\Delta t)$. The residual error for a candidate η is then defined as

$$\varepsilon_k(\eta) = d_k - (\eta d_{k-1} - d_{k-2}) \tag{51}$$

Algorithm 2 Agumented MEKF algorithm with Notch Filter

Initialization: $\widehat{\mathbf{R}}_{0|-1} = \mathbf{E}[\mathbf{R}_0]$; $\widehat{\mathbf{b}}_{0|-1} = \mathbf{b}_0$; $\widehat{\mathbf{x}}_{f_{0|-1}} = \mathbf{x}_{f_0}$; $\mathbf{P}_{0|-1} = \mathbf{P}_0$

1: **for** k = 0, 1, 2,..., n **do**
2: *Notch Filter*
3: **Filter output:**
4: $\mathbf{a}_{f_k} = \mathbf{C}\mathbf{x}_{f_k} + \mathbf{D}\left(\mathbf{a}_{m_k} - \mathbf{a}_{c_k}\right)$
5: **State update:**
6: $\mathbf{x}_{f_{k+1}} = \mathbf{A}\mathbf{x}_{f_k} + \mathbf{B}\left(\mathbf{a}_{m_k} - \mathbf{a}_{c_k}\right)$
7: *Extended Kalman Filter*
8: **Update:**
9: $\widehat{\mathbf{a}}_{f_{k|k-1}} = \mathbf{C}\widehat{\mathbf{x}}_{f_{k|k-1}} - \mathbf{D}\widehat{\mathbf{R}}_{k|k-1}^T\mathbf{e}_3$
10: $\widehat{\psi}_{k|k-1} = -\arctan\frac{\mathbf{e}_1^T\widehat{\mathbf{R}}_{k|k-1}\mathbf{e}_2}{\mathbf{e}_2^T\widehat{\mathbf{R}}_{k|k-1}\mathbf{e}_2}$
11: $\overline{\mathbf{Z}}_k = \begin{bmatrix} \mathbf{a}_{f_k} - \widehat{\mathbf{a}}_{f_{k|k-1}} & \psi_{m_k} - \widehat{\psi}_{k|k-1} \end{bmatrix}^T$
12: $\overline{\mathbf{S}}_k = \overline{\mathbf{H}}_k\overline{\mathbf{P}}_{k|k-1}\overline{\mathbf{H}}_k^T + \overline{\mathbf{D}}_v\overline{\mathcal{R}}_k\overline{\mathbf{D}}_v^T$
13: $\overline{\mathbf{K}}_k = \overline{\mathbf{P}}_{k|k-1}\overline{\mathbf{H}}_k^T\overline{\mathbf{S}}_k^{-1}$
14: $\widehat{\mathbf{R}}_{k|k} = \widehat{\mathbf{R}}_{k|k-1}\exp\left((\overline{\mathbf{E}}_1\overline{\mathbf{K}}_k\overline{\mathbf{Z}}_k)_\times\right)$
15: $\widehat{\mathbf{b}}_{k|k} = \widehat{\mathbf{b}}_{k|k-1} + \overline{\mathbf{E}}_2\overline{\mathbf{K}}_k\overline{\mathbf{Z}}_k$
16: $\widehat{\mathbf{x}}_{f_{k|k}} = \widehat{\mathbf{x}}_{f_{k|k-1}} + \overline{\mathbf{E}}_3\overline{\mathbf{K}}_k\overline{\mathbf{Z}}_k$
17: $\overline{\mathbf{P}}_{k|k} = (\mathbf{I}_{(3N+6)\times(3N+6)} - \overline{\mathbf{K}}_k\overline{\mathbf{H}}_k)\overline{\mathbf{P}}_{k|k-1}$
18: **Predict:**
19: $\widehat{\boldsymbol{\omega}}_{k|k} = \boldsymbol{\omega}_{m_k} - \widehat{\mathbf{b}}_{k|k}$
20: $\widehat{\mathbf{R}}_{k+1|k} = \widehat{\mathbf{R}}_{k|k}\exp\left((\widehat{\boldsymbol{\omega}}_{k|k})_\times\Delta t\right)$
21: $\widehat{\mathbf{b}}_{k+1|k} = \widehat{\mathbf{b}}_{k|k}$
22: $\widehat{\mathbf{x}}_{f_{k+1|k}} = \mathbf{A}\widehat{\mathbf{x}}_{f_{k|k}} - \mathbf{B}\widehat{\mathbf{R}}_{k|k}^T\mathbf{e}_3$
23: $\overline{\mathbf{P}}_{k+1|k} = \overline{\mathbf{F}}_k\overline{\mathbf{P}}_{k|k}\overline{\mathbf{F}}_k^T + \overline{\mathbf{B}}_w\overline{\mathcal{Q}}_k\overline{\mathbf{B}}_w^T$
24: **end for**

In [17], a Least Mean Square (LMS) is utilized to estimate η in real time, i.e.,

$$\begin{aligned}\widehat{\eta}_{k+1} &= \widehat{\eta}_k - \lambda\left.\frac{\partial\varepsilon_k^2(\eta)}{\partial\eta}\right|_{\widehat{\eta}_k} \\ &= \widehat{\eta}_k + \lambda d_{k-1}\varepsilon_k(\widehat{\eta}_k)\end{aligned} \tag{52}$$

where λ is the adaptation gain. The estimated $\widehat{\eta}_{k+1}$ can be directly used in (35) to construct the notch filter in real time, forming an adaptive notch filter, and also in (40) and (45) to update the system matrix (i.e. $\mathbf{A}, \mathbf{B}, \mathbf{C}$ and $\mathbf{D}$) used in augmented MEKF.

One problem with the frequency estimation method in (52) is that, it requires to know the vibration noise d, which is apparently not measurable in the actual system. In this work, we estimate dominant noise frequency (i.e. η) from the reconstructed vibration noise signal. Recalling the accelerometer model (13b), the actual vibration noise can be rewritten as

$$\mathbf{d}_k = \mathbf{a}_{m_k} + \mathbf{g}_k - \mathbf{a}_{c_k} - \mathbf{n}_{a_k} \tag{53}$$

Accordingly, the reconstructed vibration noise can be obtained as follows

$$\widehat{\mathbf{g}}_{k|k} = \widehat{\mathbf{R}}_{k|k}^T\mathbf{e}_3 \tag{54a}$$

$$\widehat{\mathbf{d}}_k = \mathbf{a}_{m_k} + \widehat{\mathbf{g}}_{k|k} - \mathbf{a}_{c_k} \tag{54b}$$

Furthermore, to mitigate the effect of measurement noise $\mathbf{n}_{a_k}$ and noise frequency components other than the dominant noise, a low-pass filter (or band-pass filter) is implemented to limit the reconstructed vibration noise $\widehat{\mathbf{d}}_k$ within a prescribed frequency range. The resulting frequency estimation algorithm is summarized in **Algorithm. 3**.

Putting all the notch filter, augmented EKF and the adaptive frequency estimation together produces the completed algorithm, whose structure is seen in Fig. 3. We should highlight that, there are two places where the notch filter is used: one is the notch filter

Algorithm 3 Adaptive frequency estimator

Initialization: $\lambda = \lambda_0, \widehat{\boldsymbol{\eta}}_0 = \boldsymbol{\eta}_0$

1: **for** $k = 2, 3, ..., n$ **do**
2: $\widehat{\mathbf{d}}_k = \mathbf{a}_{m_k} + \widehat{\mathbf{g}}_{k|k} - \mathbf{a}_{c_k}$
3: $\widehat{\mathbf{d}}_{f_k} = LPF[\widehat{\mathbf{d}}_k]$
4: $\boldsymbol{\varepsilon}_k = \mathbf{d}_{f_k} + \mathbf{d}_{f_{k-2}} - \widehat{\boldsymbol{\eta}}_k\mathbf{d}_{f_{k-1}}$
5: $\widehat{\boldsymbol{\eta}}_{k+1} = \widehat{\boldsymbol{\eta}}_k + \lambda\mathbf{d}_{f_{k-1}}\boldsymbol{\varepsilon}_k$
6: **end for**

structure (in state space form together with other state such as attitude and gyro bias) within the augmented MEKF and the other one is notch filter external to the augmented MEKF and is used to filter the accelerometer measurements.

VI. Application and Experiments

To verify the proposed attitude estimation algorithms, experiments are carried out on a three-axis gimbal system shown in Fig.4. The gimbal system is mounted on a host quadrotor UAV for imaging stabilization. The gimbal comprises an endpoint camera, whose attitude is to be estimated and controlled, and three joints that are actuated by three direct drive motors and can respectively rotate along the yaw, roll and pitch axis. A MEMS IMU (MPU6000) containing a 3-axis gyro and a 3-axis accelerometer is soldered on the camera electronics rigidly to provide measurements of camera angular rate, pitch and roll angles. The yaw measurement is computed from the host vehicle attitude and the gimbal forward kinematics [2].

We inspect the performance of the different types of attitude estimation algorithms on the gimbal system in the presence of narrow-band noise. In parallel to the attitude estimation algorithm, the gimbal system also runs an active attitude controller that tracks a commanded attitude in real time, using the attitude estimate of the estimation algorithms under investigation. The estimation algorithm has its attitude propagation step (i.e. Line 11 - Line 13 in **Algorithm. 1** or Line 20 - Line 22 in **Algorithm. 2**) running at a rate of $2000Hz$, which is also the rate of the attitude feedback controller, and its update step (i.e. Line 4 - Line 9 in **Algorithm. 1** or Line 10 - Line 18 in **Algorithm. 2**) running at $50Hz$, which is the sampling rate of the accelerometer and yaw measurements. The notch filter (i.e. Line 5 and Line 7 in **Algorithm. 2**) and adaptive frequency estimator (i.e. **Algorithm. 3**) also run at $50Hz$ if present. All algorithms are implemented on a low-end microcontroller equivalent to STM32F30x with a main frequency of $72Mhz$. In the experiments, we intentionally add a sinusoidal signal with the proper frequency and amplitude to the accelerometer measurements, to emulate the narrow-band vibration noise as shown in Fig. 1. For the sake of simplicity and the computational limitation, we consider the narrow-band noise in only one channel (i.e. channel X of the accelerometer measurements which corresponds to the pitch direction of the camera attitude), so only channel X of the accelerometer measurements are contaminated by the synthesized narrow-band noise.

We conduct four experiments, incrementally validating each component of the proposed attitude estimation algorithm. They are respectively described as follows.

- *Experiment 1*: An ordinary MEKF (i.e. **Algorithm. 1**) without any augmentation nor notch filter, is implemented to estimate the attitude. The synthesized narrow-band noise is a sinusoidal signal with frequency $2.5Hz$ and amplitude of $1g$.
- *Experiment 2*: An ordinary MEKF (i.e. **Algorithm. 1**) without any augmentation is implemented to estimate the attitude, but a notch filter external to MEKF is used to filter the accelerometer measurements. The synthesized narrow-band noise is the same as that of *Experiment 1* and accordingly, the notch filter has its parameters as $\omega_0 = 2.5Hz, \alpha = 1, \beta = 0.7, \Delta t = 0.02$ (see (33)).
- *Experiment 3*: An augmented MEKF with notch filter augmentation (i.e. **Algorithm. 2**) is implemented to estimate the attitude, and the notch filter external to MEKF is also used to filter the

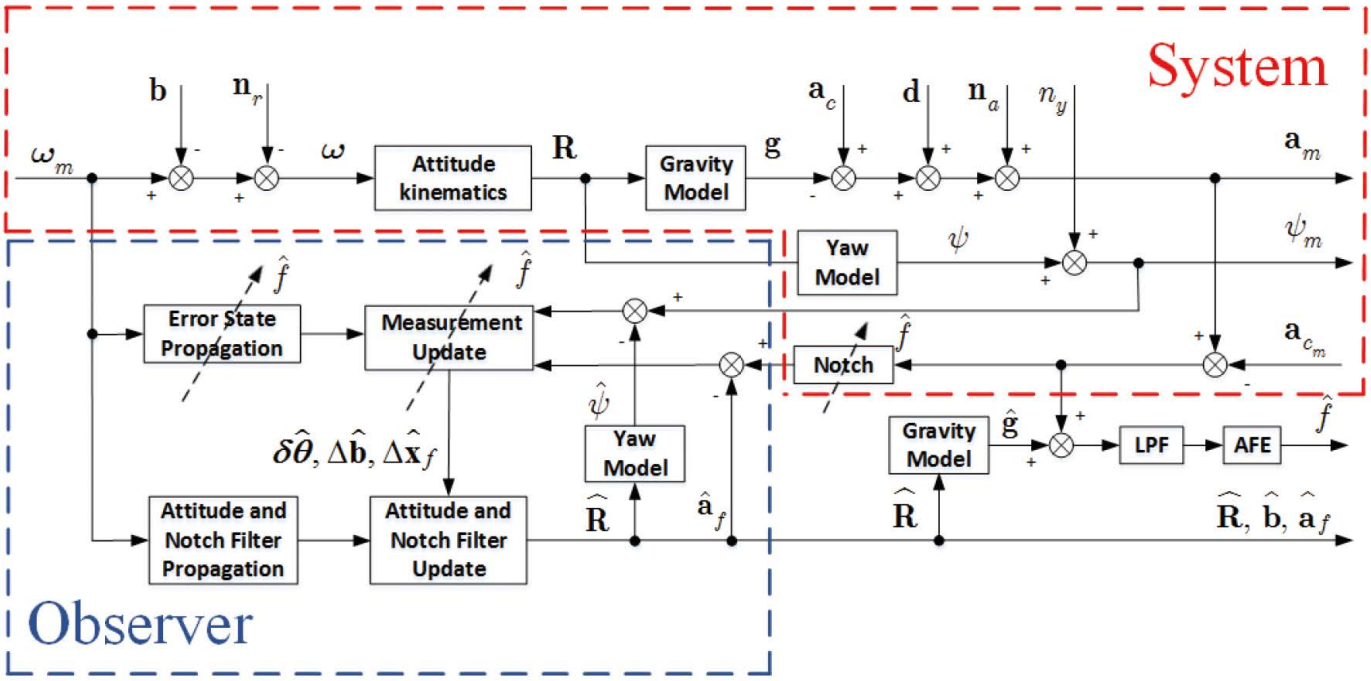

Fig. 3. Block diagram of augmented MEKF with adaptive noise frequency estimation and compensation

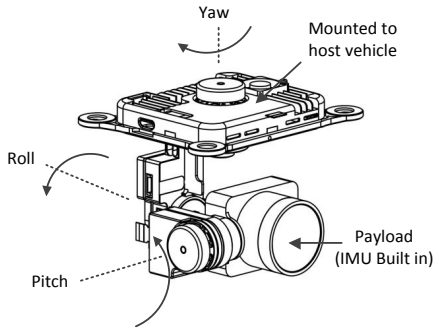

Fig. 4. Schematic of the 3-axes gimbal system (Courtesy of DJI).

accelerometer measurements. The narrow-band noise and notch filter parameters are identical to those of *Experiment 2*.

- *Experiment 4*: An augmented MEKF with notch filter augmentation (i.e. **Algorithm. 2**) is implemented to estimate the attitude, the notch filter external to MEKF is used to filter the accelerometer measurements, and the adaptive frequency estimator (i.e. **Algorithm. 3**) is employed to estimate the noise dominant frequency (the full version of Fig. 3). Different from the first three experiments where the synthesized narrow-band noise has a constant frequency and amplitude, we intentionally change the noise dominant frequency to different values (in the range of $2 \sim 4Hz$) every a few minutes. To account for the unknown and time-varying nature of the noise dominant frequency, the adaptive frequency estimator is applied. It runs at the same frequency of the augmented MEKF and the external notch filter (i.e. $50Hz$), and produces the estimate of noise dominant frequency in real time. The estimated dominant frequency $\widehat{\omega}_0$ (instead of the ground truth ω_0) is then used in (35) to construct the external notch filter in real time and also to update the system matrix of augmented MEKF (i.e. (40) and (45)). The adaptation gain λ in (52) is set to 0.005.

Again, we should mention that in all the four experiments, the synthesized narrow-band noise is only added to the X channel of accelerometer measurements (so the augmented MEKF, external

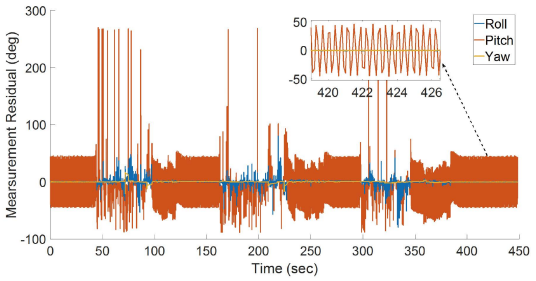

(a)

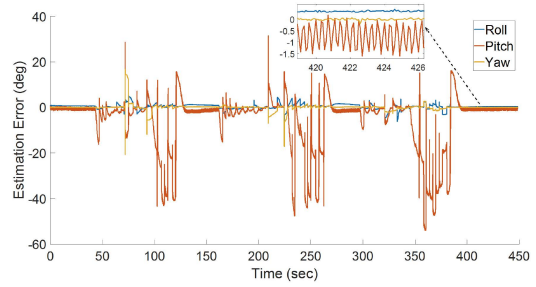

(b)

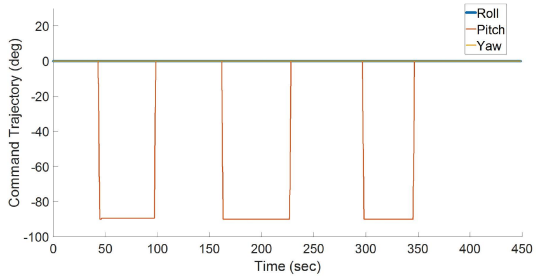

(c)

Fig. 5. Experiment 1: ordinary MEKF without notch filter nor augmentation. (a) Measurement residual. (b) Estimation error. (c) Command trajectory.

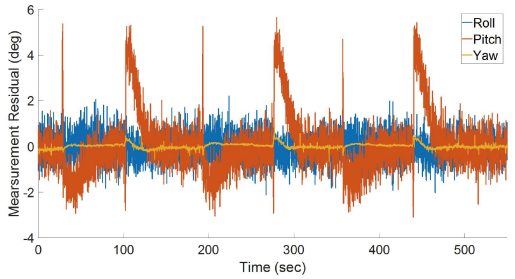

(a)

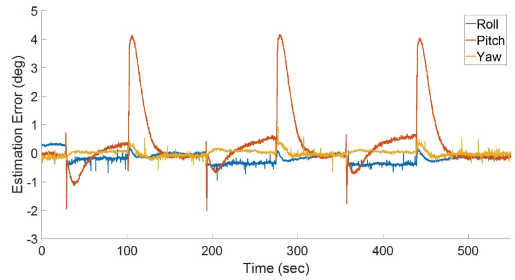

(b)

Fig. 6. Experiment 2: ordinary MEKF with notch filter but no augmentation. (a) Measurement residual. (b) Estimation error.

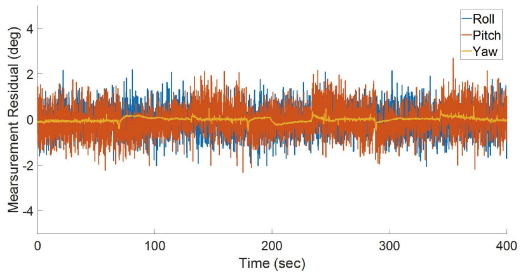

(a)

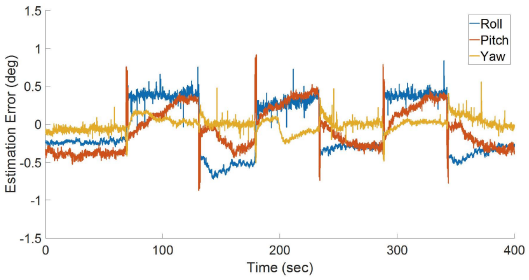

(b)

Fig. 7. Experiment 3: augmented MEKF with know notch filter and in the presence of narrow-band noise with known dominant noise. (a) Measurement residual. (b) Estimation error.

notch filter and adaptive frequency estimator are only implemented in that channel while ordinary MEKF is used for the other two channels) and the gimbal system runs an active controller that constantly tracks the commanded attitude using attitude estimate produced by the attitude estimation algorithm under investigation. The commanded attitude used in the four experiments are a pitch command from zero to -90° every several ten seconds to trigger the attitude estimation error (if any). Since the attitude commands are specified by human operator via a remote controller, they are not ensured exact the same throughout all the four experiments. An example of the attitude command is shown in Fig. 5(c).

To evaluate the effectiveness of the different attitude estimation algorithms used in the four experiments, we use two performance metrics: 1) the measurement residual (i.e. the vector $\mathbf{Z}_k$ in **Algorithm. 1** or $\overline{\mathbf{Z}}_k$ in **Algorithm. 2**) which indicates the deviation between the a-priori estimate of the observer output and their actual measurement. When the vibration noise is completely compensated, the measurement noise will be white and the measurement residual will be mean zero according to the Kalman filter theory. Note that we project the four-dimension $\overline{\mathbf{Z}}_k$ in **Algorithm. 2** to three Euler angles for intuitive comparison. 2) the error between the a-posteriori attitude estimate $\mathbf{R}_{k|k}$ and the ground truth attitude, which can approximately computed by the gimbal forward kinematics. This error is referred as "estimation error" in the following discussion. To provide an accurate attitude measurement for evaluating the algorithms in this paper, the gimbal forward kinematic parameters are calibrated by the method in [2].

Fig. 5 shows the results of the first experiment (i.e. ordinary MEKF without notch filter nor augmentation). We can see that when the camera moves to -90°, the MEKF diverges and the measurement residual are oscillatory at the noise dominant frequency due to the unmodelled narrow-band noise.

Fig. 6 illustrates results of the second experiment (i.e. ordinary MEKF with notch filter but no augmentation). Compared to the first experiment, measurement residual in Fig. 6(a) and estimation error in Fig. 6(b) suffer from no such sinusoidal noise since the external notch filter effectively attenuates the narrow-band noise in the accelerometer X-axis. The notch filter, however, introduces considerable time delay and causes a transient measurement residual (i.e. Fig. 6(a)) around 5° on pitch direction every time the camera pitch moves from zero to -90° or back forth. Similarly, the pitch estimation error (i.e. Fig. 6(b)) has a transient response around 4° before convergence. Indeed, an overshoot and a nuisance transient response over 40 secs is clearly observed from the video captured by the camera. Because no filters are implemented on the other two accelerometer channel (i.e. Y and Z channel) and yaw measurement, there are no such transient response in roll and yaw measurement residual, as well as their estimation error.

Results of the third experiment (i.e. augmented MEKF with known notch filter) are shown in Fig. 7. In Fig. 7(a), it is seen that the measurement residual of all three angles are almost identical even though the accelerometer measurement in X channel is filtered by a notch filter. The smooth and zero-mean measurement residual suggests that the augmented EKF converges fast throughout the camera movement and also effectively compensates the delay induced by the notch filter. Due to the residual kinematics calibration error [2], static estimation error of about 0.5° can be seen on roll and pitch, as shown in Fig. 7(b). The estimation error is indeed zero-mean with negligible transient response, because of the zero-mean measurement residual. As a result, the attitude response exhibits no nuisance overshoot in the captured video.

Finally, results of the fourth (i.e. augmented MEKF with adaptive notch filter) are presented in Fig. 8. It is seen in Fig. 8(c) that the estimated frequency quickly (i.e. within 0.5 sec) converges to the ground truth value. Furthermore, the measurement residual, shown in Fig. 8(a), is nearly zero mean, similar to that in the third experiment. Although in this case the pitch measurement residual is slightly more noisy than that of the third experiment due to the noisy frequency estimation, the estimated attitude shown in Fig. 8(b), is almost the same as the third experiment, suffering from no narrow-band noise nor overshoot.

Table. I summarizes the results of the four variants of MEKF. In this table, we inspect their maximum estimation error, average convergence time and whether they oscillate or diverge. The convergence time is the period from the time when the pitch command is received by the gimbal to the time when the attitude correction (i.e. $\delta\widehat{\boldsymbol{\theta}}_{k|k}$) is less than 0.01°. Note that this convergence time takes into account the delay of both estimation and control. From this table, we can see that the baseline MEKF does not even converge. With an external

Observers	Maximum Estimation Error (deg)	Average Convergence Time (sec)	Oscillation	Divergence
Ordinary MEKF without notch filter nor augmentation	53.88	N/A	Y	Y
Ordinary MEKF with notch filter but no augmentation	4.16	49.65	N	N
Augmented MEKF with known notch filter	0.92	2.13	N	N
Augmented MEKF with adaptive notch filter	1.1	2.67	N	N

TABLE I
OBSERVERS PERFORMANCE COMPARISON

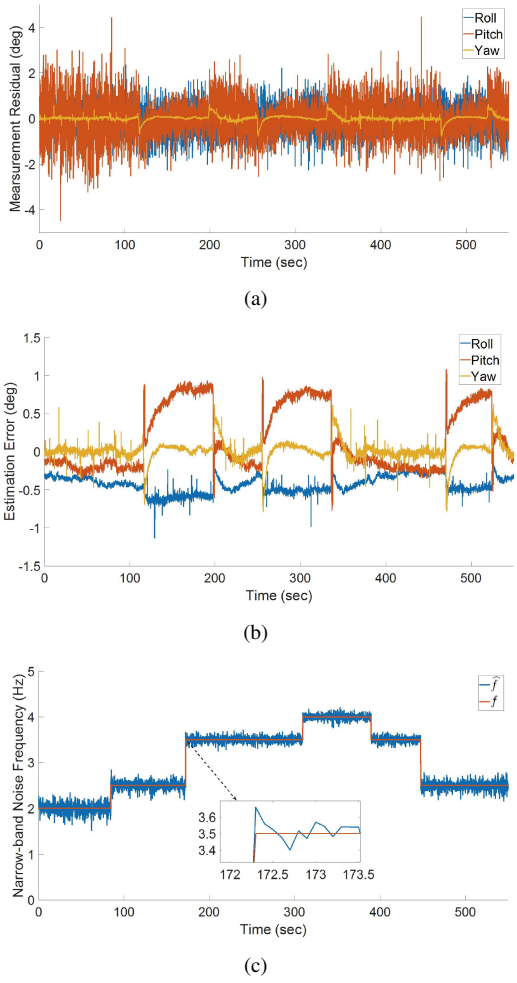

Fig. 8. Experiment 4: augmented MEKF with adaptive notch filter and in the presence of narrow-band noise with time-varying dominant noise. (a) Measurement residual. (b) Estimation error. (c) Estimated noise frequency versus the ground truth value.

notch filter, the MEKF converges but has a very long (i.e. near 50 seconds) transient response and a significant overshoot. In contrast, our proposed augmented MEKF can effectively estimate the gimbal attitude with negligible overshoot and very small convergence time (i.e. less than 3 seconds), even with time-varying dominant frequency in the noise.

VII. CONCLUSION AND FUTURE WORK

In this paper, we posed the problem of the IMU-based attitude estimation in the presence of narrow-band noise, a common problem in gimbal system due to the complicated aerodynamic effects of the robot and hostile environments where they operate. An augmented MEKF algorithm, based on multiplicative EKF framework, with a notch filter whose notch frequency is adaptively estimated, was proposed and derived on $SO(3)$. The proposed algorithm with one channel augmentation is implemented and verified on a three-axis gimbal system. The main advantage of the proposed scheme is that it effectively attenuates narrow-band noise with unknown and time-varying dominant frequency while inducing negligible delay in the attitude estimate. Future work should concentrate on development of computationally efficient algorithms and platforms with more computation power to compensate vibration noises for all three channels and with multiple narrow bands, and to form a complete and practical solution for field use.

REFERENCES

[1] X. Lyu, H. Gu, Y. Wang, Z. Li, S. Shen and F. Zhang, "Design and implementation of a quadrotor tail-sitter VTOL UAV," in *Proc. of the IEEE Intl. Conf. on Robotics and Automation (ICRA)*, Singapore, Singapore, May 2017, pp. 3924-3930

[2] F. Zhang, "Simultaneous Self-calibration of Nonorthogonality and Nonlinearity of Cost-effective Multi-axis Inertially Stabilized Gimbal Systems," *IEEE Robotics and Automation Letters*, vol. 3, no. 1, pp. 132-139, Jan. 2018.

[3] A. M. Shkel, "Type I and type II micromachined vibratory gyroscopes." in *Position, Location, And Navigation Symposium, 2006 IEEE/ION*, 2016, pp. 586 - 593

[4] D. Shaeffer, "MEMS inertial sensors: A tutorial overview," *IEEE Communications Magazine* vol. 51, no. 4, pp. 100-109, Apr. 2013.

[5] R. Mahony, V. Kumar and P. Corke, "Multirotor Aerial Vehicles: Modeling, Estimation, and Control of Quadrotor," *IEEE Robotics and Automation magazine*, vol.19, no.3, pp. 20-32, Sep. 2012.

[6] R. Mahony, T. Hamel and J. Pflimlin, "Complementary filter design on the special orthogonal group SO(3)," in *Proc. of the 44th IEEE Conference on Decision and Control*, Seville, Spain, Dec. 2005, pp. 1477-1484.

[7] T. Bailey, J. Nieto, J. Guivant, M. Stevens and E. Nebot, "Consistency of EKF-SLAM Algorithm," in *Proc. Of the IEEE/RSJ Intl. Conf. on Intelligent Robots and Systems*, Beijing, China, Oct. 2006, pp. 3562-3568.

[8] M. Li and A. Mourikis, "High-precision, consistent EKF-based visual-inertial odometry," *The International Journal of Robotics Research*, vol. 32, no. 6, pp. 690-711, 2013.

[9] S. Weiss, M. Achtelik, S. Lynen, M. Chli and R. Siegwart, "Real-time onboard visual-inertial state estimation and self-calibration of MAVs in unknown environments," in *Proc. of the IEEE Intl. Conf. on Robotics and Automation*, Saint Paul, MN, USA, May 2012, pp. 957-964.

[10] G. Klein and D. Murray, "Parallel Tracking and Mapping for Small AR Workspaces," in *Proc. of the 6th IEEE and ACM Intl. Symposium on Mixed and Augmented Reality*, Nara, Japan, Nov. 2007, pp. 225-234.

[11] Smith. G.L. and Schmidt. S.F., "The Application of Statistical Filter Theory to Optimal Trajectory Determination Onbosrd a Circumlunar Vehicle," *AAS Meeting*, Reprint 61-92, Aug. 1961.

[12] J. Crassidis, F. Markley and Y. Cheng, "Survey of Nonlinear Attitude Estimation Methods," *Journal of Guidance, Control, and Dynamics*, vol. 30, no. 1, 2007.

[13] N. Trawny and S. Roumeliotis, "Indirect Kalman Filter for 3D Attitude Estimation," University of Minnesota, Dept. of Comp. Sci. & Eng, Tech. Rep. 2005-002, Mar. 2005.

[14] F. Markley and J. Crassidis, *Fundamentals of Spacecraft Attitude Determination and Control*, Springer, New York, NY, 2014.

[15] F. Markley, "Attitude Error Representations for Kalman Filtering," *Journal of Guidance, Control, and Dynamics*, vol. 26, no. 2, pp. 311-317, 2003.

[16] J. Crassidis and F. Markley, "Unscented Filtering for Spacecraft Attitude Estimation," *Journal of Guidance, Control, and Dynamics*, vol. 26, no. 4, pp. 536-542, 2003.

[17] K. Sebesta and N. Boizot, "A Real-Time Adaptive High-Gain EKF, Applied to a Quadcopter Inertial Navigation System," *IEEE Transactions on Industrial Electronics*, vol. 61, no, 1, pp. 495-503, Jan. 2014.
[18] S. Sarkka and A. Nummenmaa, "Recursive Noise Adaptive Kalman Filtering by Variational Bayesian Approximations," *IEEE Transactions on Automatic Control*, vol. 54, no. 3, pp. 596-600, Mar. 2009.
[19] H. Qian, W. Huang, L. Qian and C. Shen, "Robust extended Kalman filter for attitude estimation with multiplicative noises and unknown external disturbances," IET Control Theory & Applications, vol. 8, no, 15, pp. 1523-1536, Oct. 2014.
[20] A. Kumar and J. Crassidis, "Colored-Noise Kalman Filter for Vibration Mitigation of Position/Attitude Estimation Systems," in *Proc. of the AIAA Guidance, Navigation and Control Conference and Exhibit*, Hilton Head, SC, USA, Aug. 2007.
[21] R. Lozano, P. Castillo, P. Garcia and A. Dzul, "Robust prediction-based control for unstable delay systems: Application to the yaw control of a mini-helicopter," *Automatica*, vol. 40, no. 4, pp. 603-612, 2004.
[22] R. Sanz, P. Garcia, P. Castillo and P. Albertos, "Time-delay compensation using inertial measurement sensors for quadrotor control systems," in *Proc. of the 17th Intl. Conference on Information Fusion*, Salamanca, Spain, Jul. 2014, pp. 1-6.
[23] Q. Jia, "Disturbance Rejection Through Disturbance Observer With Adaptive Frequency Estimation," *IEEE Transaction on Magnetics*, vol. 45, no. 6, pp. 2675-2678, Jun. 2009.
[24] R. M. Murray, Z. Li and S. S. Sastry, *A Mathematical Introduction to Robotic Manipulation*, Boca Raton, FL, USA: CRC Press, 1994.
[25] F. Bullo and R. Murray, "Proportional derivative (pd) control on the euclidean group," in European Control Conference, vol. 2, pp. 1091-1097, 1995
[26] E.J. Lefferts, F.L. Markley, and M.D. Shuster, "Kalman Filtering for Spacecraft Attitude Estimation," *Journal of Guidance, Control, and Dynamics* vol. 5, no. 5, pp. 417-429, 1982.
[27] G. Allibert, D. Abeywardena, M. Bangura, and R. Mahony. "Estimating body-fixed frame velocity and attitude from inertial measurements for a quadrotor vehicle." in *Proc. of the IEEE Conf. on Control Application (CCA)*, Juan Les Antibes, France, Oct. 2014, pp. 978-983.
[28] J. P. Hespanha, *Linear systems theory*, Princeton university Press, 2009.

Guozheng Lu received the B.S. degree in Automation from Harbin Institute of Technology, Harbin, China, in 2016. Since joining Dajiang Innovations (DJI) in 2016, he has been a Control Engineer with emphasis on estimation, dynamics, control, calibration, and their engineering applications to commercial aerial robots.

Fu Zhang is an Assistant Professor of the Department of Mechanical Engineering at the University of Hong Kong. He received his B.E. degree in Automation from the University of Science and Technology of China (USTC), China, and the Ph.D. degree in Controls from the University of California, Berkeley, USA. His research focuses on mechatronic systems and robotics, including design, calibration, estimation, control, and perception.